Cell Reports



# Reward learning improves social signal processing in autism model mice

## Graphical abstract

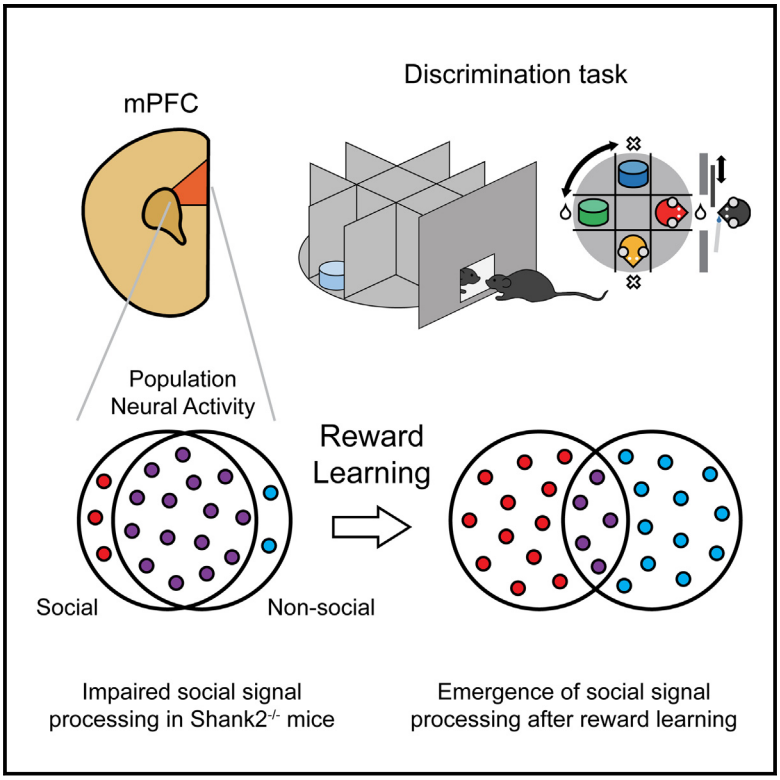


## Highlights

- Social and reward signals are conjunctly represented in the mPFC
- Reward signal processing is intact in the mPFC of *Shank2*$^{-/-}$ mice
- Social signal processing is disrupted in the mPFC of *Shank2*$^{-/-}$ mice
- Reward learning restores impaired mPFC social signal processing in *Shank2*$^{-/-}$ mice

## Authors

Joowon Kim, Min Whan Jung, Doyun Lee

## Correspondence

mwjung@kaist.ac.kr (M.W.J.),
leedoyun@ibs.re.kr (D.L.)

## In brief

Kim et al. demonstrate that reward learning can restore impaired social signal processing in the medial prefrontal cortex of *Shank2*-knockout mice. This finding suggests that reward-based behavioral therapy for autism has potential to enhance social signal processing at the neuronal level.

Kim et al., 2023, Cell Reports *42*, 113228
October 31, 2023 
https://doi.org/10.1016/j.celrep.2023.113228

CellPress

Cell Reports

CellPress
OPEN ACCESS

Report

# Reward learning improves social signal processing in autism model mice

Joowon Kim,[1,2] Min Whan Jung,[2,3,4,*] and Doyun Lee[1,5,*]
[1]Center for Cognition and Sociality, Institute for Basic Science, Daejeon 34126, Korea
[2]Graduate School of Medical Science and Engineering, Korea Advanced Institute of Science and Technology, Daejeon 34141, Korea
[3]Department of Biological Sciences, Korea Advanced Institute of Science and Technology, Daejeon 34141, Korea
[4]Center for Synaptic Brain Dysfunction, Institute for Basic Science, Daejeon 34141, Korea
[5]Lead contact
*Correspondence: mwjung@kaist.ac.kr (M.W.J.), leedoyun@ibs.re.kr (D.L.)
https://doi.org/10.1016/j.celrep.2023.113228

## SUMMARY

Social and reward signal processing and their association are critical elements of social motivation. Despite the use of reward learning to improve the social interactions of patients with autism spectrum disorder (ASD), the underlying neural mechanisms are unknown. Here, we found different yet conjunct neuronal representations of social and reward signals in the mouse medial prefrontal cortex (mPFC). We also found that social signal processing is selectively disrupted, whereas reward signal processing is intact in the mPFC of *Shank2*-knockout mice, a mouse model of ASD. Furthermore, reward learning not only allows *Shank2*-knockout mice to associate social stimuli with reward availability, but it also rescues the impaired social signal processing. These findings provide insights into the neural basis for the therapeutic use of reward learning in ASD.

## INTRODUCTION

Social interactions are often intertwined with rewarding experiences, giving rise to social motivation. Lack of social motivation is a defining trait of autism spectrum disorder (ASD) and one of its diagnostic criteria.[1] Social signal processing and reward-based learning are two important elements of social motivation. Therefore, understanding how social and reward processing are altered in ASD is important to understand the neural basis of ASD, but our understanding of this issue at the neuronal level is limited. Currently, there is no definite treatment for ASD, but behavioral interventions that utilize positive reinforcement are applied to patients with ASD to improve their social behavioral performance.[2–4]

The goal of behavioral therapy for ASD patients is to generate a lasting improvement in social behavior even when rewards are no longer provided. In addition, one of the key questions is whether reward-based therapy can facilitate the transition of improved behaviors to novel social situations that were not encountered during therapy. This raises the question of whether reward learning improves the brain's ability to process social information in general. Although the human psychosocial interventions appear to be successful, albeit limited, in improving social behaviors in ASD patients, it is unclear whether the positive effects of behavioral therapy are due to improved neural processing of social signals or simply due to reinforced behavior in previously learned social situations. Therefore, understanding whether and how reward learning improves social signal processing in ASD would be important for developing strategies for treating ASD. However, to the best of our knowledge, we have little understanding of this matter at the neuronal level.

The medial prefrontal cortex (mPFC) is a central neuroanatomical hub for social and reward circuits, and it integrates multiple types of information to modulate complex social behaviors.[5–8] The mPFC, which is connected with other social areas, including the nucleus accumbens, the ventral tegmental area, the amygdala, and the hippocampal CA1,[9–14] shows selective responses to social stimuli.[15–17] Manipulation of the mPFC modulates social motivation and even rescues the sociability of ASD model mice.[9,18–21] In addition, the mPFC is a key component of the reward circuit, encodes reward information, and modulates reward-seeking behavior.[22,23] Therefore, the mPFC offers the best opportunity to investigate possible relationships between social and reward signal processing. However, it is unclear whether these two forms of information are processed by separate or overlapping neural populations and how their responses influence each other. Furthermore, how social and reward signal processing are selectively and differently affected in ASD and whether social representations emerge at the neuronal level following reward learning remain to be investigated.

In this study, we developed a novel behavioral paradigm that allows us to investigate social and reward processing simultaneously, and we found that reward learning can rescue social signal processing in the mPFC that is selectively impaired in *Shank2*-knockout (*Shank2*$^{-/-}$) mice, a widely used mouse model of ASD.[24–26]

## RESULTS

### Social signal processing is selectively impaired in *Shank2*$^{-/-}$ mice

To elucidate how social information is processed and represented and to investigate how reward learning affects social signal processing in the mPFC of wild-type (WT) and *Shank2*$^{-/-}$ mice, we designed a social versus non-social odor discrimination task. The subjects were placed in front of a turntable, separated by a window, with four cues: two social cues and two non-social cues. The task was designed with reward association in mind, where one social cue and one non-social cue would be associated with reward upon the introduction of a lick port, so that each cue would be of different social category and different reward category. All subjects underwent viral vector injection and GRIN lens implantation in the mPFC for *in vivo* calcium imaging before participating in behavioral training (Figure 1A).

To investigate social signal processing in the mPFC before reward learning, the subjects went through passive presentation, i.e., the cues were presented without any reward (Figure 1B). Upon the opening of the window, the subjects were presented with one cue, randomly selected from the four cues, for 4 to 6 s. After the cue presentation, the window was closed and an inter-trial interval of approximately 8 s was followed. The duration of cue presentation was randomized between trials to reduce anticipatory licking during the reward learning phase. We monitored the activity of mPFC neurons expressing GCaMP6f using *in vivo* calcium imaging while the mice were performing the task (Figure 1C).

Mean calcium responses to the cues were overall similar between WT and *Shank2*$^{-/-}$ mice, suggesting that the mean activity level of the neurons was not different; however, the number of mPFC neurons that were activated or inhibited in response to social cues was smaller in *Shank2*$^{-/-}$ mice than WT mice (Figures S1A and S1B). The proportions of "social" neurons, which responded differentially to social versus non-social odor stimuli (Figure 1D), were 21.2% ± 3.4% and 4.0% ± 0.9% in WT and *Shank2*$^{-/-}$ mice, respectively, which differed significantly from each other (Figure 1E).

Next, we tested whether the population activity pattern of mPFC neurons distinguished between social and non-social odors. We trained a support vector machine (SVM) decoder to classify social and non-social odor trials and calculated the decoding accuracy using the leave-one-out cross-validation procedure. In WT mice, the accuracy of neuronal population decoding of social versus non-social cues was near chance level until about 0.5 s after the opening of the window, and it rapidly increased to a plateau. Conversely, such an increase in the decoding accuracy was not observed in *Shank2*$^{-/-}$ mice (Figure 1F). The accuracy of neuronal population decoding of social versus non-social cues was significantly lower in *Shank2*$^{-/-}$ mice than WT mice: 72.1% ± 3.2% and 48.9% ± 1.5% correct decoding accuracy in WT and *Shank2*$^{-/-}$ mice, respectively (Figure 1G). The difference in SVM decoding was not due to a difference in the number of cells used for population decoding (Figure S2A). Furthermore, population decoding using matched number of cells between WT and *Shank2*$^{-/-}$ mice showed concurring results (Figures S2B).

In addition, we investigated how the neural representation of social information at the population level changed upon repeated exposures to the same cues. The accuracy of population decoding increased with repeated exposures to the cues for 3 consecutive days in WT mice (Figures 1H and 1I), consistent with previous observations in that WT mice displayed an experience-dependent refinement of social representation across days.[12] In contrast, in *Shank2*$^{-/-}$ mice, population decoding accuracy decreased with familiarization (Figures 1J and 1K). Altogether, these results show that social and non-social odors can be discriminated by the neuronal activity in the mPFC in WT mice, but this ability is impaired in *Shank2*$^{-/-}$ mice.

### *Shank2*$^{-/-}$ mice can learn the association between social stimuli and reward availability

After the passive presentation, the subjects went through reward learning. The task structure was identical to the passive presentation except for a lick port situated in front of the subjects (Figure 2A). The mice were trained to lick in response to only one social and one non-social cue and to refrain from licking in response to the other cues. The addition of the reward component to one of the social and non-social cues apportioned each cue to different social and reward contexts (Figure 2B).

Although it took an average of 6.4 additional sessions for *Shank2*$^{-/-}$ mice to reach the performance criterion of 80% correct rate (Figures 2C and 2D), the performance after reaching the criterion was comparable between WT and *Shank2*$^{-/-}$ mice (Figure 2E). When the performance was assessed separately for the social and non-social trials, there was no difference between WT and *Shank2*$^{-/-}$ mice (Figure 2E). This suggests that, once learned, *Shank2*$^{-/-}$ mice can distinguish between social and non-social cues as proficiently as WT mice, and that they retain the potential ability to associate odor cues with reward availability regardless of the social category of the cue.

Interestingly, we observed that *Shank2*$^{-/-}$ mice did not exhibit a bias toward licking, which is typically observed in Go/No-Go task in WT mice (Figures 2F, S3A, and S3B). *Shank2*$^{-/-}$ mice also displayed a higher frequency of prolonged licking after receiving reward compared to WT mice (Figures 2G–2I). Altogether, these results show that *Shank2*$^{-/-}$ mice are capable of forming stimulus-reward associations for both social and non-social stimuli, although the learning rate was slower compared to WT mice.

### Social signal processing is improved following reward learning in *Shank2*$^{-/-}$ mice

Our task design enabled us to examine the neural representations of both social and reward information, both at the level of individual neurons and the level of neuronal population during the reward task. In well-trained mice, the proportions of social cells, neurons that discriminate between social and non-social cues, were 25.6% ± 3.7% and 14.9% ± 3.9% in WT and *Shank2*$^{-/-}$ mice, respectively (Figure 3A). The proportions of reward cells, neurons that discriminate between reward-associated and non-reward-associated cues, were 17.4% ± 2.7% and 23.8% ± 2.5% in WT and *Shank2*$^{-/-}$ mice, respectively (Figure 3A). Although social and reward neurons were substantially different populations, they showed significant association, i.e., the overlap between

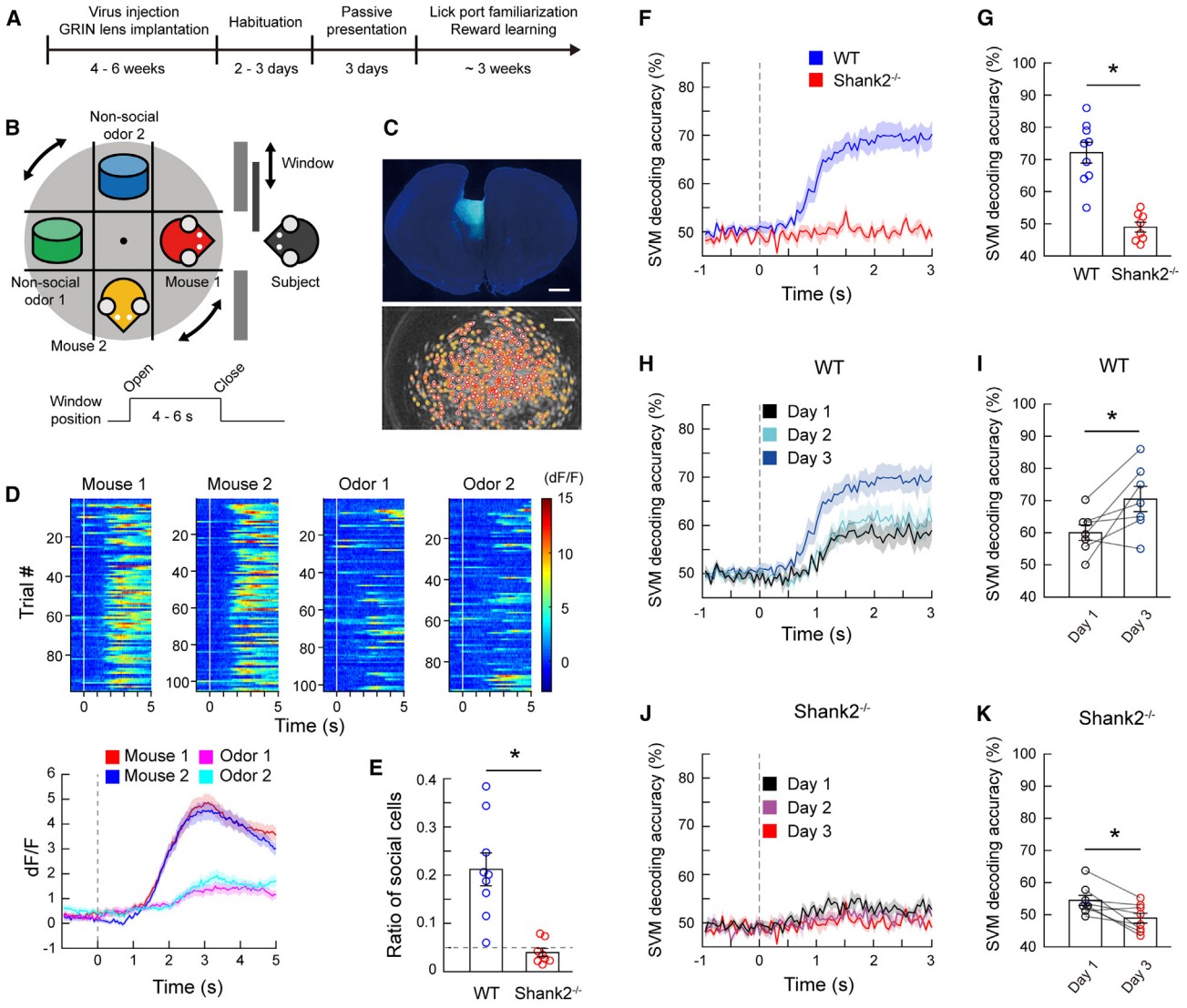


**Figure 1. Social signal processing is selectively impaired in *Shank2*$^{-/-}$ mice**

(A) Schematic of the training schedule.

(B) Top: schematic of the behavioral setup during passive presentation. Bottom: task structure.

(C) Histology of the imaged area (top) and the detected regions of interest (ROIs) (bottom) for an example mouse (scale bar: 1 mm and 100 μm for top and bottom panels, respectively).

(D) An example of a social cell. Heatmap of the neural activity of an example social cell (top) and the mean activity for each cue of an example social cell (bottom). Time 0 indicates window opening.

(E) Comparison of the ratios of social cells in WT and *Shank2*$^{-/-}$ mice during passive presentation (unpaired t test, n = 9 for WT, n = 8 for *Shank2*$^{-/-}$, $p < 0.001$).

(F) SVM decoding accuracies of social information in WT and *Shank2*$^{-/-}$ mice. Time 0 indicates window opening.

(G) Comparison of the SVM decoding accuracies of social information in WT and *Shank2*$^{-/-}$ mice (unpaired t test, n = 9 for WT, n = 8 for *Shank2*$^{-/-}$, $p < 0.001$).

(H) SVM decoding accuracies for three passive presentation sessions in WT mice. Time 0 indicates window opening.

(I) Comparison of the SVM decoding accuracies on day 1 and day 3 in WT mice (paired t test, n = 7, $p = 0.033$).

(J) SVM decoding accuracies for three passive presentation sessions in *Shank2*$^{-/-}$ mice. Time 0 indicates window opening.

(K) Comparison of the SVM decoding accuracies on day 1 and day 3 in *Shank2*$^{-/-}$ mice (paired t test, n = 8, $p = 0.011$).

the two populations was higher than that expected by chance, suggesting conjunctive coding between the two representations (Chi-square test with neurons pulled across all mice, $p < 0.001$ in WT, $p < 0.001$ in *Shank2*$^{-/-}$ mice). There were also neurons that were modulated by the combination of social and reward categories but not by social or reward categories alone, i.e., neurons with significant interaction effect (Figure 3A). The proportions of social and reward cells were not significantly different between WT and *Shank2*$^{-/-}$ mice after reward learning (Figures 3B and 3C).

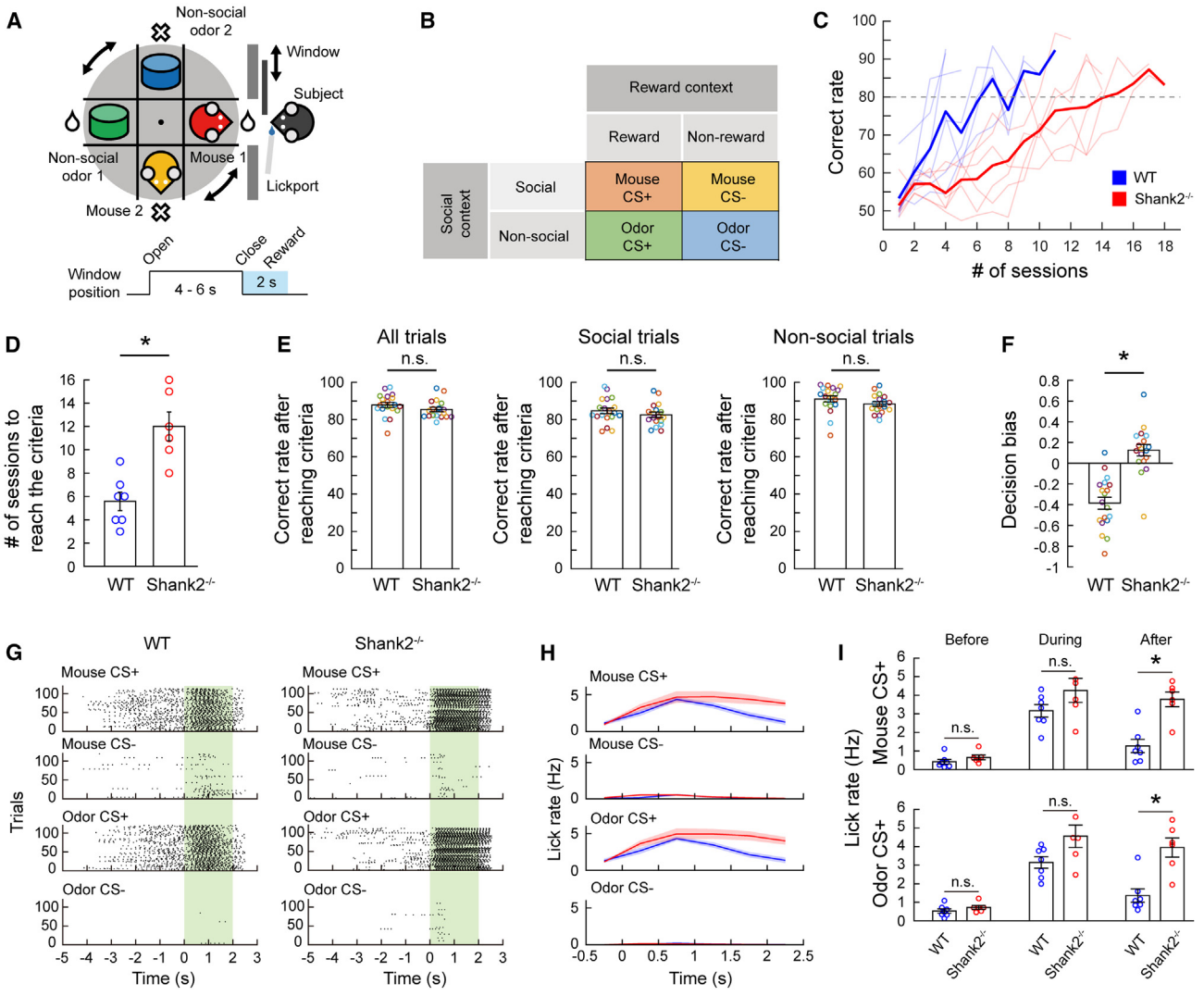


**Figure 2. Comparison of behavioral performance on the reward task between WT and *Shank2*$^{-/-}$ mice**

(A) Schematic of the behavioral setup during reward learning.

(B) Table of cues by their social and reward context.

(C) Time courses for reward learning in WT and *Shank2*$^{-/-}$ mice. Mean time courses are in opaque colors, and individual time courses are in semi-transparent colors. The dashed line indicates the high-performance criterion.

(D) Comparison of the number of sessions to reach the behavioral criteria in WT and *Shank2*$^{-/-}$ mice (5.6 ± 0.8 sessions for WT, 12.0 ± 1.2 sessions for *Shank2*$^{-/-}$; unpaired t test, n = 7 for WT, n = 6 for *Shank2*$^{-/-}$, $p < 0.001$).

(E) Left: comparison of the correct rate for all trials (unpaired t test, n = 19 sessions in 7 WT mice, n = 18 sessions in 6 *Shank2*$^{-/-}$ mice, $p = 0.19$). Center: social trials (unpaired t test, n = 19 sessions in 7 WT mice, n = 18 sessions in 6 *Shank2*$^{-/-}$ mice, $p = 0.31$). Right: non-social trials (unpaired t test, n = 19 sessions in 7 WT mice, n = 18 sessions in 6 *Shank2*$^{-/-}$ mice, $p = 0.20$). Circles of the same color indicate sessions from the same mouse.

(F) Comparison of the decision bias of WT and *Shank2*$^{-/-}$ mice (unpaired t test, n = 19 sessions for WT, n = 18 sessions for *Shank2*$^{-/-}$, $p < 0.001$). Circles of the same color indicate sessions from the same mouse.

(G) The raster plots of licking responses of well-trained WT (left) and *Shank2*$^{-/-}$ (right) mice, aligned to the beginning of the response period. The response period is the 2 s between window closing and the end of the trial, indicated by shaded green.

(H) Licking rates (mean ± SEM) of WT (blue) and *Shank2*$^{-/-}$ (red) mice (n = 7 for WT, n = 6 for *Shank2*$^{-/-}$), aligned to the beginning of the response period.

(I) Comparison of the lick rates before, during, and after the response period in mouse CS + trials (left) and odor CS + trials (right) in WT and *Shank2*$^{-/-}$ mice (unpaired t test, n = 7 for WT, n = 6 for *Shank2*$^{-/-}$, $p = 0.23$, $p = 0.14$, $p < 0.001$ before, during and after the response period in mouse CS + trials, respectively, and $p = 0.26$, $p = 0.053$, $p = 0.0015$ before, during, and after the response period in odor CS + trials, respectively).

Next, we examined the neural representations of social and reward information at the neuronal population level. The decoding accuracy of social information was higher in WT mice than in *Shank2*$^{-/-}$ mice (Figures 3D and 3E), while the decoding accuracy of reward information was comparable in WT and *Shank2*$^{-/-}$ mice (Figures 3F and 3G). The decoding accuracy of social information

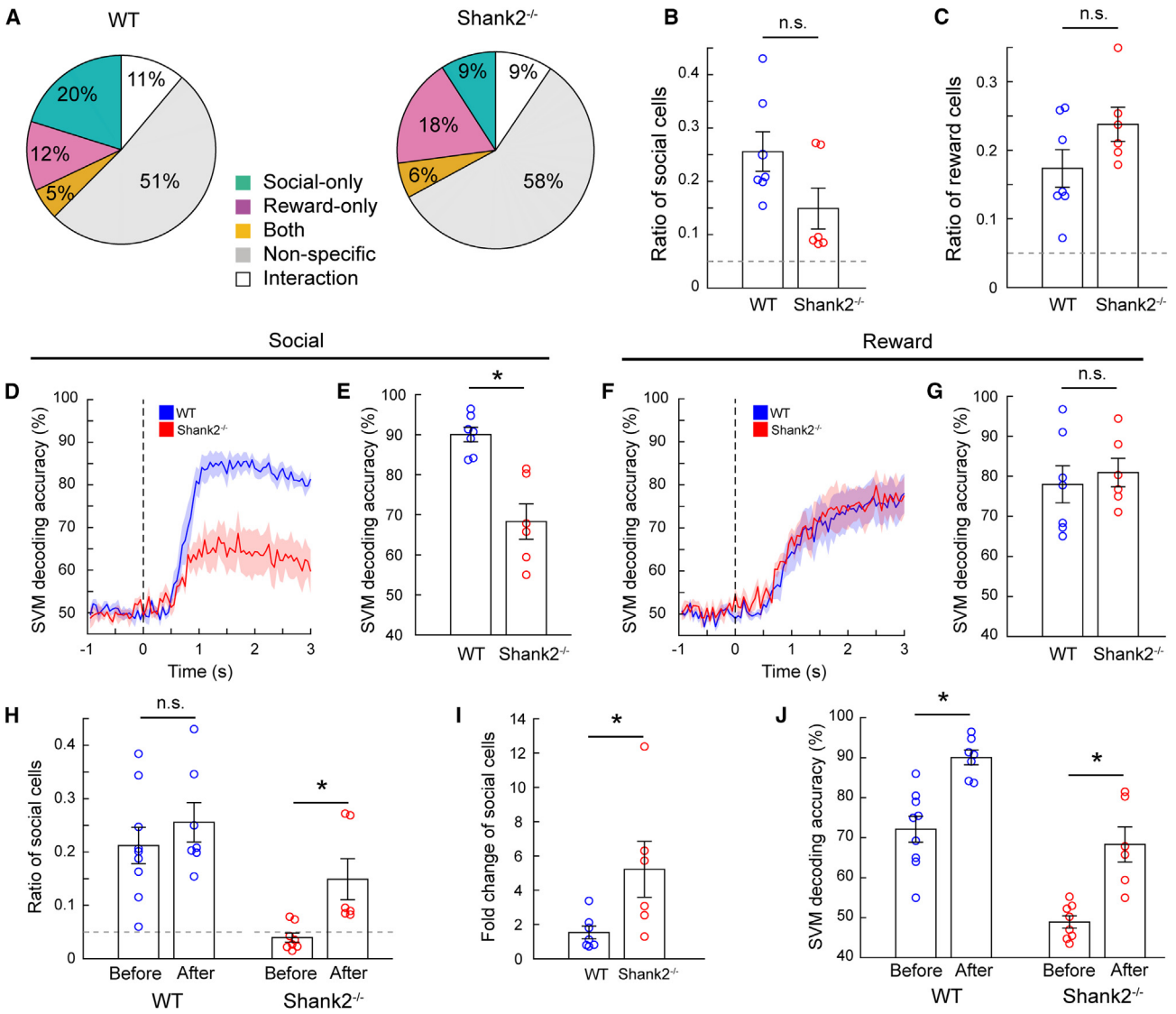


**Figure 3. Social signal processing is rescued following reward learning in *Shank2*$^{-/-}$ mice**

(A) The ratio of social, reward and both cells in WT (left) and *Shank2*$^{-/-}$ (right) mice (n = 7 for WT, n = 6 for *Shank2*$^{-/-}$).

(B) Comparison of the ratio of social cells after reward learning in WT and *Shank2*$^{-/-}$ mice (unpaired t test, n = 7 for WT, n = 6 for *Shank2*$^{-/-}$, p = 0.071).

(C) Comparison of the ratio of reward cells after reward learning in WT and *Shank2*$^{-/-}$ mice (unpaired t test, n = 7 for WT, n = 6 for *Shank2*$^{-/-}$, p = 0.11).

(D) SVM decoding accuracies for social information in WT and *Shank2*$^{-/-}$ mice. Time 0 indicates window opening.

(E) Comparison of the SVM decoding accuracies for social information (unpaired t test, n = 7 for WT, n = 6 for *Shank2*$^{-/-}$, p < 0.001).

(F) SVM decoding accuracies for reward information in WT and *Shank2*$^{-/-}$ mice. Time 0 indicates window opening.

(G) Comparison of the SVM decoding accuracies for reward information (unpaired t test, n = 7 for WT, n = 6 for *Shank2*$^{-/-}$, p = 0.63).

(H) Comparison of the ratio of social cells before and after reward learning in WT (left) and *Shank2*$^{-/-}$ (right) mice (unpaired t test, n = 9 for before, n = 7 for after, p = 0.40 in WT; n = 8 for before, n = 6 for after, p = 0.0078 in *Shank2*$^{-/-}$).

(I) Comparison of the fold change in the ratio of social cells in WT and *Shank2*$^{-/-}$ mice (unpaired t test, n = 7 for WT, n = 6 for *Shank2*$^{-/-}$, p = 0.037).

(J) Comparison of the SVM decoding accuracies for social information before and after reward learning in WT (left) and *Shank2*$^{-/-}$ (right) mice (unpaired t test, n = 9 for before, n = 7 for after, p < 0.001 in WT; n = 8 for before, n = 6 for after, p < 0.001 in *Shank2*$^{-/-}$).

was higher when calculated within reward trials than non-reward trials in both WT and *Shank2*$^{-/-}$ mice (Figures S4A–S4F). These results suggest that while *Shank2*$^{-/-}$ mice have deficiencies in social signal processing, their reward signal processing is similar to that of WT mice.

Compared to passive presentation, the ratio of social cells did not increase significantly in WT mice, but in *Shank2*$^{-/-}$ mice, the ratio of social cells increased significantly (Figure 3H). The fold change of the ratio of social cells was significantly greater in *Shank2*$^{-/-}$ mice compared to WT mice (Figure 3I). The decoding

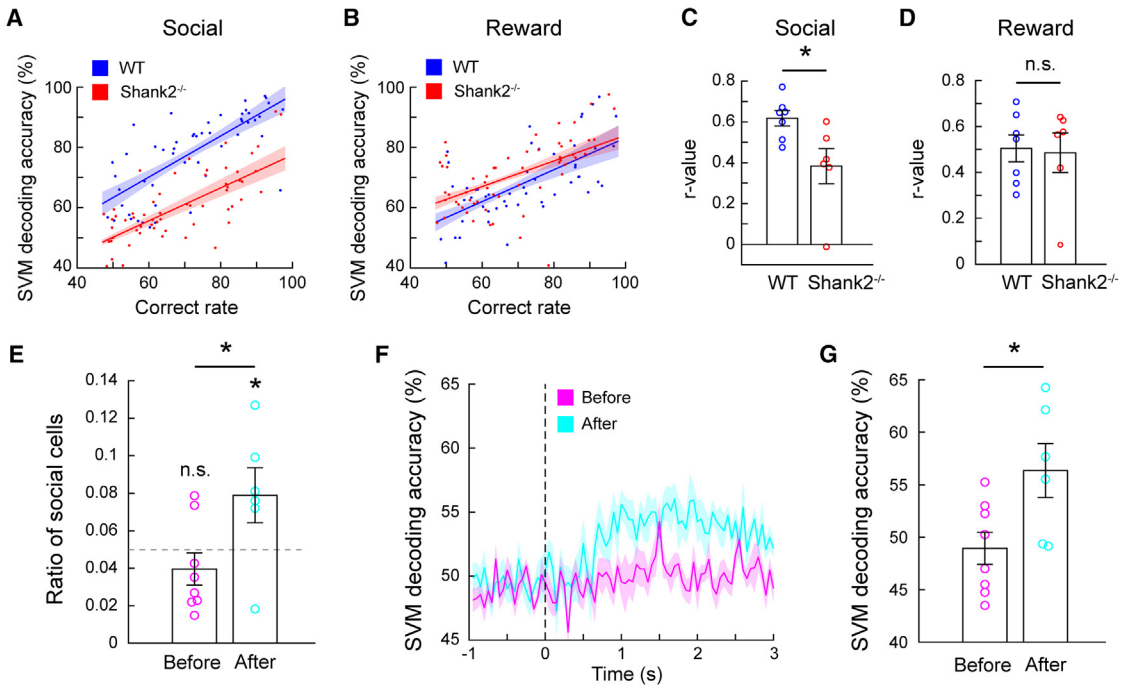


**Figure 4. Emerged social representation is maintained with significant stability**

(A) Correlation between SVM decoding accuracies for social information and behavioral performance ($r = 0.72$, $p < 0.001$ for WT, $r = 0.73$, $p < 0.001$ for *Shank2*$^{-/-}$ mice). Dots for each session from 7 WT and 6 *Shank2*$^{-/-}$ mice. Fitting lines are mean ± SEM across regression lines for each mouse.

(B) Correlation between SVM decoding accuracies for reward information and behavioral performance ($r = 0.65$, $p < 0.001$ for WT, $r = 0.60$, $p < 0.001$ for *Shank2*$^{-/-}$ mice).

(C) Comparison of the correlation coefficients of discrimination index (DI) values for social information in 2 consecutive days in WT and *Shank2*$^{-/-}$ mice (unpaired t test, n = 7 for WT, n = 6 for *Shank2*$^{-/-}$, $p = 0.023$).

(D) Comparison of the correlation coefficients of DI values for reward information in 2 consecutive days in WT and *Shank2*$^{-/-}$ mice (unpaired t test, n = 7 for WT, n = 6 for *Shank2*$^{-/-}$, $p = 0.86$).

(E) Comparison of the ratio of social cells during passive presentation before and after reward learning in *Shank2*$^{-/-}$ mice (unpaired t test, n = 8 for before, n = 6 for after, $p = 0.030$, $p < 0.001$ compared to chance).

(F) SVM decoding accuracies for social information before and after reward learning in *Shank2*$^{-/-}$ mice. Time 0 indicates window opening.

(G) Comparison of the SVM decoding accuracies for social information before and after reward learning in *Shank2*$^{-/-}$ mice (unpaired t test, n = 8 for before, n = 6 for after, $p = 0.023$).

accuracy of social information increased in both WT and *Shank2*$^{-/-}$ mice (Figure 3J). The number of cells used for population decoding was comparable between WT and *Shank2*$^{-/-}$ mice (Figure S4G). Furthermore, population decoding using matched number of cells between WT and *Shank2*$^{-/-}$ mice showed concurring results (Figure S4H). Paired analysis at the cellular and population level in WT and *Shank2*$^{-/-}$ mice showed concurring results (Figures S5A–S5D). Altogether, these results show that social and reward information are represented by different yet overlapping subsets of mPFC neurons, and social cells, which were absent during passive presentation, emerged after reward learning in *Shank2*$^{-/-}$ mice.

## Stable social representation emerged during reward learning

Next, we investigated how social and reward information emerged during reward learning. The population decoding accuracy of social information increased along with the behavioral performance of the reward task (Figure 4A). Specifically, the decoding accuracy of social information in *Shank2*$^{-/-}$ mice increased at a similar rate as WT mice, starting from chance level. These results suggest that there is a correlation between the progression of reward learning and the emergence of neuronal representation of social information. The improvement in decoding accuracy of reward information during reward learning was similar in WT and *Shank2*$^{-/-}$ mice, suggesting intact reward processing in *Shank2*$^{-/-}$ mice (Figure 4B).

In well-trained mice, we investigated the stability of social and reward cells by comparing discrimination index values on 2 consecutive days. The stability of social and reward information was above chance in both WT and *Shank2*$^{-/-}$ mice, with the stability of social information being higher in WT mice compared to *Shank2*$^{-/-}$ mice, whereas the stability of reward information was comparable (Figures 4C, 4D, S6A, and S6B). These results indicate that social and reward information are encoded with stable representations in the mPFC and that reward circuit is intact in *Shank2*$^{-/-}$ mice.

To examine whether the emerged social signal processing in *Shank2*$^{-/-}$ mice following reward learning is maintained even after the reward is removed, the subjects underwent

passive presentation after reward learning. The ratio of social cells was significantly higher compared to that of passive presentation before reward learning and to chance level (Figure 4E). The population decoding of social information was also higher during passive presentation after reward learning compared to that of before reward learning (Figures 4F and 4G). These results suggest a possibility that the social signal processing acquired through reward learning persists even in the absence of reward.

## DISCUSSION

In this study, we developed a novel behavioral paradigm to investigate social and reward signal processing simultaneously. Combined with *in vivo* calcium imaging, we observed a social signal processing circuit, different from, yet conjunct to the reward circuit in the mPFC. We showed that the reward circuit was intact, and social signal processing was selectively impaired in *Shank2*$^{-/-}$ mice. After reward learning, i.e., associating reward to social and non-social cues, social signal processing was partially rescued in *Shank2*$^{-/-}$ mice, and the effect persisted after the removal of reward.

The use of reward learning as a behavior modification technique has been shown to be effective in treating ASD.[27] However, the neural mechanisms underlying the improvement are still not well understood. A crucial question in ASD research is whether reward learning can enhance the brain's ability to process social information in general, i.e., apart from the improvement of the limited social interactions used during reward learning, of which our understanding has been limited so far. Our results demonstrate the evidence that neuronal processing of social information can be enhanced through reward learning, offering new insights into the therapeutic potentials of reward learning for the treatment of ASD.

Impairment in social reward processing, i.e., associating reward value with social stimuli, has been hypothesized to be the underlying cause of social deficit in ASD, on which current behavior therapies such as the applied behavior analysis are based.[28,29] However, the discrepancies of impairment between social reward and non-social reward processing in ASD patients, such as the difference in the deficit in reward learning between social rewards and monetary rewards, have been difficult to explain.[30] Previous studies have crudely indicated a specialized and exclusive channel for social signal processing apart from non-social signal processing.[9,31] However, it was unclear why manipulating the classical reward circuit affected sociability.[5,32] It could be speculated that social reward processing involves interactions between social and reward representations, where the former is selectively impaired, while the latter is relatively intact in ASD, and that their significant overlap influences each other so that social signal processing is modulated by the reward circuit and vice versa to contribute to social motivation. Our results revealed that both the social and reward neurons are present in the mPFC and that they display a noticeable degree of overlap. These observations support the mPFC as a potential domain where social and reward information are integrated, thus mediating social reward processing.

The distinction between social and reward components was quite ambiguous in conventional and widely used methods such as the three-chamber test.[9,15,24] It was difficult to ascertain whether the interpretation or the consequence of a manipulation was indeed specifically of social or reward component. The behavioral paradigm we have employed in this study enabled us to clearly distinguish social and reward components at the cellular and the population levels. To further investigate the function of social and reward representations on the modulation of social behaviors, jointly and separately, specific labeling and manipulation of social and reward representations could be possible with the application of calcium integrators and *in vivo* two-photon optogenetic stimulation.[33,34] Differences in the projection and the molecular profiles of social and reward neurons in the mPFC could also be traced to examine their roles in tandem with other brain regions involved in social signal processing.

Our observation of different representations of social and reward information and their association, as well as the rescuing effect of social representation by reward learning provides insights to the pathophysiology and the therapeutic applications of ASD.

### Limitations of the study

In the present study, we observed remarkable improvements in social representation in the mPFC of mice during a reward association task. Interestingly, this enhancement was maintained even after the removal of reward. Although the results are significant, their impact is moderate. It is of great interest to determine whether our approach will produce more substantial results in juvenile mice, of which the neural circuits have greater plasticity. Additionally, considering that the mice were trained only for two additional sessions after reaching the performance criterion, a longer period of training may result in even better improvements in social signal processing after the removal of reward. Our study also tested the effect of reward leaning in just one type of autism model mice, so it is necessary to confirm whether the results are replicable in other autism model mice.

Given that our model organism is the mouse, which is well known to rely on olfaction as its primary sensory modality for social recognition,[35] we identified social cells by comparing neuronal responses to real mice with those to neutral odors. Even though the subject mice discriminate between stimulus mice and non-social odor stimuli based on olfactory characteristics, these two types of stimuli may differ in many non-social aspects such as the intensity, composition of the smell, and inherent preferences of the subject mice. That mPFC neurons of *Shank2*$^{-/-}$ mice could not differentiate between the stimulus mice and the non-social odors prior to reward learning indicates that *Shank2*$^{-/-}$ mice have an impairment in social versus non-social discrimination in the mPFC. However, it remains ambiguous whether the emerged ability of discriminating between stimulus mice and non-social odors via reward learning can be solely attributed to social versus non-social discrimination. A more comprehensive comparison, perhaps involving neural responses to the stimulus mice against various control stimuli across different sensory modalities, could have addressed this issue. This remains an unaddressed concern in our study.

Finally, we did not test whether the rescue of social signal processing at the neuronal level is sufficient to improve social behavior such as an increased preference for interacting with social stimuli. Considering the limited improvement in the social

signal processing after the removal of reward, behavioral enhancement could also be marginal.

## STAR★METHODS

Detailed methods are provided in the online version of this paper and include the following:

- KEY RESOURCES TABLE
- RESOURCE AVAILABILITY
  - Lead contact
  - Materials availability
  - Data and code availability
- EXPERIMENTAL MODEL AND SUBJECT DETAILS
  - Animals
- METHOD DETAILS
  - Surgery
  - Behavioral apparatus
  - Behavioral paradigm
  - Training protocol
  - *In vivo* calcium imaging
  - Behavioral performance
- QUANTIFICATION AND STATISTICAL ANALYSIS
  - Identification of social and reward cells
  - SVM decoding of social and reward information
  - Statistics

## SUPPLEMENTAL INFORMATION

Supplemental information can be found online at https://doi.org/10.1016/j.celrep.2023.113228.

## ACKNOWLEDGMENTS

We thank Eunjoon Kim for the helpful comments on the manuscript. This work was supported by the Institute for Basic Science (IBS), Center for Cognition and Sociality (IBS-R001-D2 to D.L.), and Center for Synaptic Brain dysfunction (IBS-R002-G1 to M.W.J.).

## AUTHOR CONTRIBUTIONS

J.K. and D.L. conceived and designed the research. J.K. performed the experiments. J.K and D.L. wrote the analysis code. J.K. analyzed data with input from all authors. J.K. wrote the first draft. J.K., M.W.J., and D.L. contributed to the final version of the paper. M.W.J. and D.L. supervised the research.

## DECLARATION OF INTERESTS

The authors declare no competing interests.

Received: February 21, 2023
Revised: September 3, 2023
Accepted: September 21, 2023

## REFERENCES

1. Chevallier, C., Kohls, G., Troiani, V., Brodkin, E.S., and Schultz, R.T. (2012). The social motivation theory of autism. Trends Cogn. Sci. *16*, 231–239. https://doi.org/10.1016/j.tics.2012.02.007.
2. Li, T., Wang, X., Pan, J., Feng, S., Gong, M., Wu, Y., Li, G., Li, S., and Yi, L. (2016). Reward learning modulates the attentional processing of faces in children with and without autism spectrum disorder. Autism Res. *10*, 1797–1807. https://doi.org/10.1002/aur.1823.
3. Roane, H.S., Fisher, W.W., and Carr, J.E. (2016). Applied behavior analysis as treatment for autism spectrum disorder. J. Pediatr. *175*, 27–32. https://doi.org/10.1016/j.jpeds.2016.04.023.
4. Schuetze, M., Rohr, C.S., Dewey, D., McCrimmon, A., and Bray, S. (2017). Reinforcement learning in autism spectrum disorder. Front. Psychol. *8*, 2035. https://doi.org/10.3389/fpsyg.2017.02035.
5. Gunaydin, L.A., Grosenick, L., Finkelstein, J.C., Kauvar, I.V., Fenno, L.E., Adhikari, A., Lammel, S., Mirzabekov, J.J., Airan, R.D., Zalocusky, K.A., et al. (2014). Natural neural projection dynamics underlying social behavior. Cell *157*, 1535–1551. https://doi.org/10.1016/j.cell.2014.05.017.
6. Olsson, A., Knapska, E., and Lindström, B. (2020). The neural and computational systems of social learning. Nat. Rev. Neurosci. *21*, 197–212. https://doi.org/10.1038/s41583-020-0276-4.
7. Yamamuro, K., Bicks, L.K., Leventhal, M.B., Kato, D., Im, S., Flanigan, M.E., Garkun, Y., Norman, K.J., Caro, K., Sadahiro, M., et al. (2020). A prefrontal–paraventricular thalamus circuit requires juvenile social experience to regulate adult sociability in mice. Nat. Neurosci. *23*, 1240–1252. https://doi.org/10.1038/s41593-020-0695-6.
8. Yan, Z., and Rein, B. (2022). Mechanisms of synaptic transmission dysregulation in the prefrontal cortex: pathophysiological implications. Mol. Psychiatry *27*, 445–465. https://doi.org/10.1038/s41380-021-01092-3.
9. Murugan, M., Jang, H.J., Park, M., Miller, E.M., Cox, J., Taliaferro, J.P., Parker, N.F., Bhave, V., Hur, H., Liang, Y., et al. (2017). Combined social and spatial coding in a descending projection from the prefrontal cortex. Neuron *171*, 1663–1677.e16. https://doi.org/10.1016/j.cell.2017.11.002.
10. Okuyama, T., Kitamura, T., Roy, D.S., Itohara, S., and Tonegawa, S. (2016). Ventral CA1 neurons store social memory. Science *353*, 1536–1541. https://doi.org/10.1126/science.aaf7003.
11. Phillips, M.L., Robinson, H.A., and Pozzo-Miller, L. (2019). Ventral hippocampal projections to the medial prefrontal cortex regulate social memory. Elife *8*, e44182. https://doi.org/10.7554/eLife.44182.
12. Dölen, G., Darvishzadeh, A., Huang, K.W., and Malenka, R.C. (2013). Social reward requires coordinated activity of nucleus accumbens oxytocin and serotonin. Nature *501*, 179–184. https://doi.org/10.1038/nature12518.
13. Hung, L.W., Neuner, S., Polepalli, J.S., Beier, K.T., Wright, M., Walsh, J.J., Lewis, E.M., Luo, L., Deisseroth, K., Dölen, G., and Malenka, R.C. (2017). Gating of social reward by oxytocin in the ventral tegmental area. Science *357*, 1406–1411. https://doi.org/10.1126/science.aan4994.
14. Kong, E., Lee, K.-H., Do, J., Kim, P., and Lee, D. (2023). Dynamic and stable hippocampal representations of social identity and reward expectation support associative social memory in male mice. Nat. Commun. *14*, 2597. https://doi.org/10.1038/s41467-023-38338-3.
15. Lee, E., Rhim, I., Lee, J.W., Ghim, J.W., Lee, S., Kim, E., and Jung, M.W. (2016). Enhanced neuronal activity in the medial prefrontal cortex during social approach behavior. J. Neurosci. *36*, 6926–6936. https://doi.org/10.1523/JNEUROSCI.0307-16.2016.
16. Levy, D.R., Tamir, T., Kaufman, M., Parabucki, A., Weissbrod, A., Schneidman, E., and Yizhar, O. (2019). Dynamics of social representation in the mouse prefrontal cortex. Nat. Neurosci. *22*, 2013–2022. https://doi.org/10.1038/s41593-019-0531-z.
17. Liang, B., Zhang, L., Barbera, G., Fang, W., Zhang, J., Chen, X., Chen, R., Li, Y., and Lin, D.T. (2018). Distinct and dynamic ON and OFF neural ensembles in the prefrontal cortex code social exploration. Neuron *100*, 700–714.e9. https://doi.org/10.1016/j.neuron.2018.08.043.
18. Yizhar, O., Fenno, L.E., Prigge, M., Schneider, F., Davidson, T.J., O'Shea, D.J., Sohal, V.S., Goshen, I., Finkelstein, J., Paz, J.T., et al. (2011). Neocortical excitation/inhibition balance in information processing and social dysfunction. Nature *477*, 171–178. https://doi.org/10.1038/nature10360.

19. Selimbeyoglu, A., Kim, C.K., Inoue, M., Lee, S.Y., Hong, A.S.O., Kauvar, I., Ramakrishnan, C., Fenno, L.E., Davidson, T.J., Wright, M., and Deisseroth, K. (2017). Modulation of prefrontal cortex excitation/inhibition balance rescues social behavior in CNTNAP2-deficient mice. Sci. Transl. Med. *9*, eaah6733. https://doi.org/10.1126/scitranslmed.aah6733.

20. Cao, W., Lin, S., Xia, Q.Q., Du, Y.L., Yang, Q., Zhang, M.Y., Lu, Y.Q., Xu, J., Duan, S.M., Xia, J., et al. (2018). Gamma oscillation dysfunction in mPFC leads to social deficits in neuroligin 3 R451C knockin mice. Neuron *97*, 1253–1260.e7. https://doi.org/10.1016/j.neuron.2018.02.001.

21. Tan, T., Wang, W., Liu, T., Zhong, P., Conrow-Graham, M., Tian, X., and Yan, Z. (2021). Neural circuits and activity dynamics underlying sex-specific effects of chronic social isolation stress. Cell Rep. *34*, 108874. https://doi.org/10.1016/j.celrep.2021.108874.

22. Otis, J.M., Namboodiri, V.M.K., Matan, A.M., Voets, E.S., Mohorn, E.P., Kosyk, O., McHenry, J.A., Robinson, J.E., Resendez, S.L., Rossi, M.A., and Stuber, G.D. (2017). Prefrontal cortex output circuits guide reward seeking through divergent cue encoding. Nature *543*, 103–107. https://doi.org/10.1038/nature21376.

23. Wang, P.Y., Boboila, C., Chin, M., Higashi-Howard, A., Shamash, P., Wu, Z., Stein, N.P., Abbott, L.F., and Axel, R. (2020). Transient and persistent representations of odor value in prefrontal cortex. Neuron *108*, 209–224.e6. https://doi.org/10.1016/j.neuron.2020.07.033.

24. Won, H., Lee, H.R., Gee, H.Y., Mah, W., Kim, J.I., Lee, J., Ha, S., Chung, C., Jung, E.S., Cho, Y.S., et al. (2012). Autistic-like social behaviour in Shank2-mutant mice improved by restoring NMDA receptor function. Nature *486*, 261–265. https://doi.org/10.1038/nature11208.

25. Chung, C., Ha, S., Kang, H., Lee, J., Um, S.M., Yan, H., Yoo, Y.E., Yoo, T., Jung, H., Lee, D., et al. (2019). Early correction of N-Methyl-D-Aspartate receptor function improves autistic-like social behaviors in adult Shank2$^{-/-}$ mice. Biol. Psychiatry *85*, 534–543. https://doi.org/10.1016/j.biopsych.2018.09.025.

26. Lee, E., Lee, S., Shin, J.J., Choi, W., Chung, C., Lee, S., Kim, J., Ha, S., Kim, R., Yoo, T., et al. (2021). Excitatory synapses and gap junctions cooperate to improve PV neuronal burst firing and cortical social cognition in Shank2-mutant mice. Nat. Commun. *12*, 5116. https://doi.org/10.1038/s41467-021-25356-2.

27. Virués-Ortega, J. (2010). Applied behavior analytic intervention for autism in early childhood: Meta-analysis, meta-regression and dose–response meta-analysis of multiple outcomes. Clin. Psychol. Rev. *30*, 387–399. https://doi.org/10.1016/j.cpr.2010.01.008.

28. Clements, C.C., Zoltowski, A.R., Yankowitz, L.D., Yerys, B.E., Schultz, R.T., and Herrington, J.D. (2018). Evaluation of the social motivation hypothesis of autism: a systematic review and meta-analysis. JAMA Psychiatr. *75*, 797–808. https://doi.org/10.1001/jamapsychiatry.2018.1100.

29. Bottini, S. (2018). Social reward processing in individuals with autism spectrum disorder: a systematic review of the social motivation hypothesis. Res. Autism Spectr. Disord. *45*, 9–26. https://doi.org/10.1016/j.rasd.2017.10.001.

30. Lin, A., Rangel, A., and Adolphs, R. (2012). Impaired learning of social compared to monetary rewards in autism. Front. Neurosci. *6*, 143. https://doi.org/10.3389/fnins.2012.00143.

31. Kelly, E., Meng, F., Fujita, H., Morgado, F., Kazemi, Y., Rice, L.C., Ren, C., Escamilla, C.O., Gibson, J.M., Sajadi, S., et al. (2020). Regulation of autism-relevant behaviors by cerebellar–prefrontal cortical circuits. Nat. Neurosci. *23*, 1102–1110. https://doi.org/10.1038/s41593-020-0665-z.

32. Walsh, J.J., Christoffel, D.J., Heifets, B.D., Ben-Dor, G.A., Selimbeyoglu, A., Hung, L.W., Deisseroth, K., and Malenka, R.C. (2018). 5-HT release in nucleus accumbens rescues social deficits in mouse autism model. Nature *560*, 589–594. https://doi.org/10.1038/s41586-018-0416-4.

33. Fosque, B.F., Sun, Y., Dana, H., Yang, C.T., Ohyama, T., Tadross, M.R., Patel, R., Zlatic, M., Kim, D.S., Ahrens, M.B., et al. (2015). Labeling of active neural circuits in vivo with designed calcium integrators. Science *347*, 755–760. https://doi.org/10.1126/science.1260922.

34. Jennings, J.H., Kim, C.K., Marshel, J.H., Raffiee, M., Ye, L., Quirin, S., Pak, S., Ramakrishnan, C., and Deisseroth, K. (2019). Interacting neural ensembles in orbitofrontal cortex for social and feeding behaviour. Nature *565*, 645–649. https://doi.org/10.1038/s41586-018-0866-8.

35. Ryan, B.C., Young, N.B., Moy, S.S., and Crawley, J.N. (2008). Olfactory cues are sufficient to elicit social approach behaviors but not social transmission of food preference in C57BL/6J mice. Behav. Brain Res. *193*, 235–242. https://doi.org/10.1016/j.bbr.2008.06.002.

36. Lopes, G., Bonacchi, N., Frazão, J., Neto, J.P., Atallah, B.V., Soares, S., Moreira, L., Matias, S., Itskov, P.M., Correia, P.A., et al. (2015). Bonsai: an event-based framework for processing and controlling data streams. Front. Neuroinform. *9*, 7. https://doi.org/10.3389/fninf.2015.00007.

37. Zhou, P., Resendez, S.L., Rodriguez-Romaguera, J., Jimenez, J.C., Neufeld, S.Q., Giovannucci, A., Friedrich, J., Pnevmatikakis, E.A., Stuber, G.D., Hen, R., et al. (2018). Efficient and accurate extraction of in vivo calcium signals from microendoscopic video data. Elife *7*, e28728. https://doi.org/10.7554/eLife.28728.

38. Sheintuch, L., Rubin, A., Brande-Eilat, N., Geva, N., Sadeh, N., Pinchasof, O., and Ziv, Y. (2017). Tracking the same neurons across multiple days in $Ca^{2+}$ imaging data. Cell Rep. *21*, 1102–1115. https://doi.org/10.1016/j.celrep.2017.10.013.

## STAR★METHODS

### KEY RESOURCES TABLE

| REAGENT or RESOURCE | SOURCE | IDENTIFIER |
|---|---|---|
| Bacterial and virus strains | | |
| pENN.AAV1.CamKII.GCaMP6f.WPRE.SV40 | Addgene | Catalog # 100834-AAV1; RRID: Addgene_100834 |
| Chemicals, peptides, and recombinant proteins | | |
| Citral | Sigma Aldrich | CAS # 5392405 |
| Isoamyl acetate | Sigma Aldrich | CAS # 123922 |
| Experimental models: Organisms/strains | | |
| Mouse: C57BL/6J | The Jackson Laboratory | #000664 |
| Mouse: *Shank2*$^{-/-}$ | Eunjoon Kim's Lab | N/A |
| Software and algorithms | | |
| MATLAB | MathWorks | N/A |
| Bonsai | Lopes et al.[36] | N/A |
| Inscopix Data Processing Software | Inscopix | N/A |
| CNMF-E | Zhou et al.[37] | N/A |
| CellReg | Sheintuch et al.[38] | N/A |
| Original code | This paper | https://doi.org/10.5281/zenodo.8352766 |

### RESOURCE AVAILABILITY

#### Lead contact

Further information and requests for resources and reagents should be directed to and will be fulfilled by the lead contact, Doyun Lee (leedoyun@ibs.re.kr).

#### Materials availability

This study did not generate new unique reagents.

#### Data and code availability

All data reported in this paper will be shared by the lead contact upon request. Custom MATLAB code for analyzing the data are available at https://doi.org/10.5281/zenodo.8352766.

### EXPERIMENTAL MODEL AND SUBJECT DETAILS

#### Animals

Behavior and imaging data were collected from 9 C57BL/6J WT male mice (The Jackson Laboratory; 2–3 months old) and 8 *Shank2*$^{-/-}$ male mice. Subject mice were housed individually after surgery. Conspecifics presented as cues were C57BL/6J WT male mice and were littermate pairs. The conspecifics used as cues were not littermates with the subject mice. The mice were maintained on a 12-h light/dark cycle with food *ad libitum*. All procedures used in this work were approved by the Institutional Animal Care and Use Committee of the Institute for Basic Science (Daejeon, South Korea).

### METHOD DETAILS

#### Surgery

The mice were anesthetized with isoflurane (1–3%) and the body temperature was maintained at 37°C with a heating pad (DC Temperature Control System, FHC Inc.). For viral injections, AAV1.CaMKII.GCaMP6f was injected to the right mPFC, at the coordinate AP -1.85, ML 0.30, DV -1.70. Two days after viral injection, a circular craniotomy of diameter 1.0 mm was made centered at the injection site and part of the cerebral cortex was removed by aspiration. A GRIN lens of diameter 1.0 mm (PPL-1043, Inscopix) was inserted on top of the injection site. A stainless steel head bar for head-fixation was attached to the cranium and was covered with dental acrylic.

#### Behavioral apparatus

Four cues were placed on a turntable (diameter of 24 cm), separated from the subject mouse by a window of size 3 (width) × 2.5 (height) cm$^2$. A stepper motor (SBC-NK245-03AT, Motorbank) was used to rotate the turntable. The window was controlled

by a servo motor (MEDS15, Makeblock Co. Ltd.). A lick port mounted on a three-axis micromanipulator and was placed in front of the subject mouse. The lick port was made of a stainless steel tube (diameter of 1.3 mm) and was controlled with a solenoid valve (161T011, NResearch Inc.) to deliver reward. The apparatus was enclosed in a 60 × 60 × 60 $cm^3$ soundproof box. The turntable, the window and the lick port were all controlled by Arduino microcontrollers and behavioral data were acquired using Bonsai.[36]

### Behavioral paradigm

Four cues were used, with two cues being male conspecifics and two cues being non-social odors. The conspecifics used for cues were head-fixed on a custom-designed mounting platform. The non-social odors used were citral (CAS # 5392405, Sigma Aldrich) and isoamyl acetate (CAS # 123922, Sigma Aldrich), diluted by 1/500 with mineral oil, placed in a dish for diffusion. Although the concentration of the odor decreased over time due to evaporation, calcium response to the odor cues was not different during the first and the second half of the session (data not shown). The cues were presented in a pseudo-random order. The window was opened for 5 ± 1 s. The opening durations were randomized between trials to minimize anticipatory licking. The inter-trial interval was approximately 8 s. During reward learning training, a lick port was placed in front of the subject mouse. After the window was closed, a tone (2 kHz) was given for 2 s to indicate the response period. A water droplet was given when the subject licked during CS + trials. Mice were not punished for incorrect lickings during CS- trials. A session consisted of about 400 trials during passive presentation and about 480 trials during reward learning.

### Training protocol

Prior to training, the subject mice were put on a water-restriction schedule and were given approximately 1 mL of water daily to maintain approximately 80% of the initial body weight. After handling, the subject mice were habituated to head-fixation in the behavioral box for 30–60 min for 2–3 days. After habituation, the subject mice went through 3 days of passive presentation, i.e., the four cues were presented passively without the lick port and reward. After passive presentation, the lick port was situated in front of the subject mice. After being familiarized to the lick ports, reward learning was commenced. The subject mice were trained to lick during the response period of the trials with cues that were associated with reward, and refrain from licking during the response period of the trials with cues that were not associated with reward. For *Shank2*$^{-/-}$ mice, after reaching the correct rate of 80%, the subject mice went through additional passive presentation sessions after training. For the 2 WT mice and the 2 *Shank2*$^{-/-}$ mice which did not reach the criterion of 80% correct rate, only passive presentation data were used.

### *In vivo* calcium imaging

GCaMP6f fluorescence in the mPFC was imaged using a miniaturized fluorescence microscope (nVoke, Inscopix). The field of view was imaged at 20 frames/sec. Motion correction was done using the Inscopix Data Processing Software (Inscopix). Fluorescence from the regions of interest (ROIs) were extracted using the MATLAB package CNMF-E[37]. Tracking the activity of the same set of neurons across multiple sessions was done using the MATLAB package CellReg.[38]

### Behavioral performance

CS + trials in which the subjects successfully licked the lick port were defined as ''hit trials''. CS + trials in which the subjects failed to lick the lick port were defined as ''miss trials''. CS- trials in which the subjects wrongfully licked the lick port were defined as ''false alarm trials''. CS- trials in which the subjects successfully refrained from licking the lick port were defined as ''correct rejection trials''. The behavioral correct rate was calculated as follows: (# of hit trials + # of correct rejection trials)/# of all trials. The d' value for the signal detection theory was calculated as follows: $_{CR}$ - $z_{miss}$, where $z_{CR}$ and $z_{miss}$ are the inverse of the standard normal cumulative distribution function of the correct rejection rate and the miss rate, respectively. The decision bias was calculated as follows: d'/2 + $z_{miss}$.

## QUANTIFICATION AND STATISTICAL ANALYSIS

### Identification of social and reward cells

To classify neurons into social and reward cells, we used two-way ANOVA with interaction (anovan in MATLAB). For passive presentation sessions, in which there was no reward, only social cells were defined. For sessions after reward learning, neurons with significant main effect were defined as social and reward neurons. Neurons with significant interaction term were excluded to rule out confounding factors in regard to social and reward interaction. Discrimination index (DI) was defined as follows: $(\mu_1 - \mu_2)/\mathrm{sqrt}((\sigma_1^2 + \sigma_2^2)/2)$, where $\mu$ and $\sigma$ represent the mean and the standard deviations of areas under calcium events during each trial type.

### SVM decoding of social and reward information

For population decoding of social and reward information, SVM decoder with a linear kernel (fitcsvm in MATLAB) with the leave-one-out cross-validation procedure was used. For each imaging session, independent SVMs were trained and tested at each time point. Specifically, each decoder was trained with the neural population activity pattern from all trials in the session except a withheld trial. Then we tested if the trained decoder classified the held-out trial into the correct category. For each session, the procedure was

repeated by withholding a different trial at a time so that the withheld trials span the entire session. Decoding accuracy was expressed as the proportion of correct classifications. For comparing the decoding accuracies between WT and *Shank2*$^{-/-}$ mice, SVM decoding was done with the area under the curve (AUC) of the calcium activity traces during the 3 s after window opening.

### Statistics

All data analysis was performed with MATLAB (MathWorks) with custom codes. A p value $<0.05$ was used as the criterion for statistical significance. All data were expressed as mean ± SEM.

**Cell Reports, Volume *42***

## Supplemental information

# Reward learning improves social signal processing in autism model mice

**Joowon Kim, Min Whan Jung, and Doyun Lee**

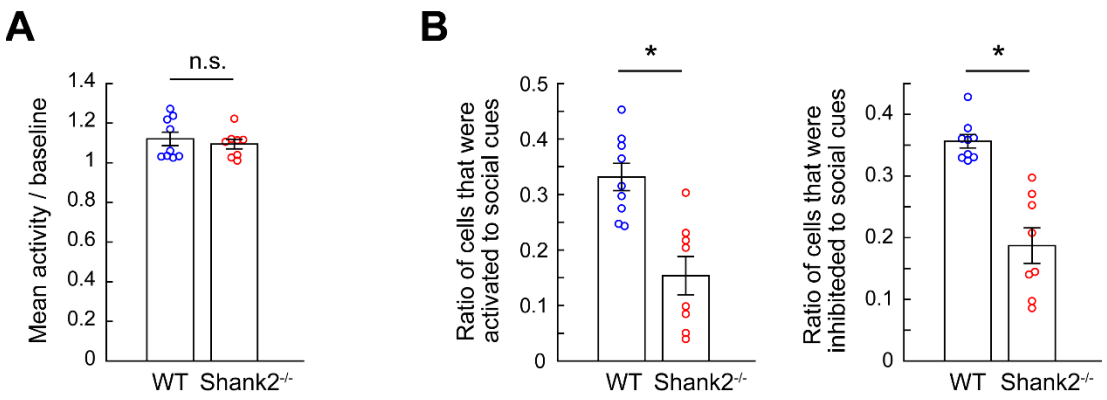


**Figure S1 Comparison of calcium responses between WT and *Shank2*$^{-/-}$ mice**

(**A**) Mean calcium responses across sessions are similar between WT and *Shank2*$^{-/-}$ mice during passive presentation (unpaired t-test, n = 9 for WT, n = 8 for *Shank2*$^{-/-}$, p = 0.56).

(**B**) A smaller fraction of neurons was activated (left, $p < 0.001$) or inhibited (right, $p < 0.001$) in response to social cues in *Shank2*$^{-/-}$ than WT mice (unpaired t-test, n = 9 for WT, n = 8 for *Shank2*$^{-/-}$).

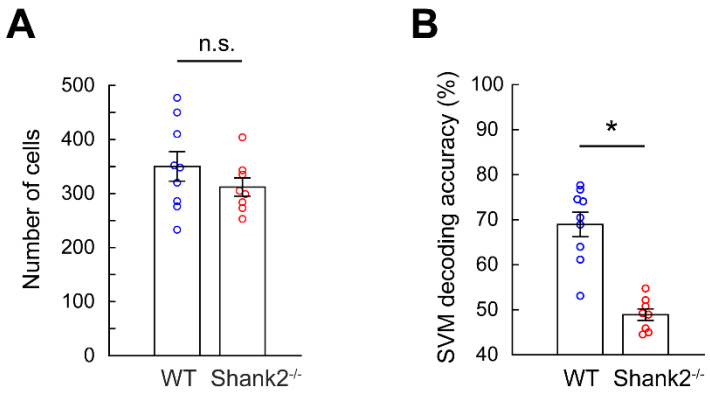


**Figure S2 Difference in the population decoding accuracies between WT and *Shank2*$^{-/-}$ mice were not due to different number of cells used for analysis.**

(**A**) Comparison of the number of cells used for SVM decoding during passive presentation in WT and *Shank2*$^{-/-}$ mice (unpaired t-test, n = 9 for WT, n = 8 for *Shank2*$^{-/-}$, p = 0.27).

(**B**) Comparison of the SVM decoding accuracies for social information during passive presentation, matching the number of cells between WT and *Shank2*$^{-/-}$ mice (unpaired t-test, n = 9 for WT, n = 8 for *Shank2*$^{-/-}$, $p < 0.001$).

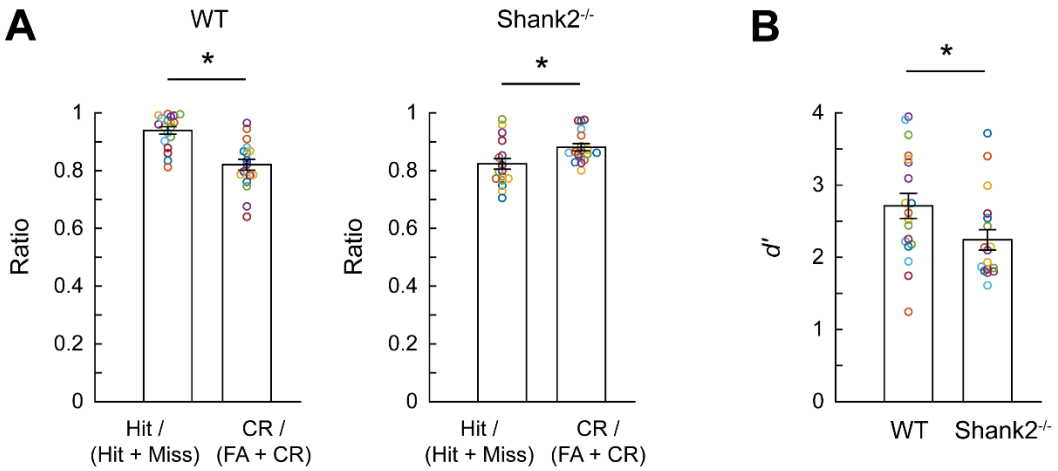


**Figure S3 A bias toward licking in WT mice is not present in *Shank2*$^{-/-}$ mice.**

(**A**) Comparison of the ratio of hit and correct rejection trials in WT (left) and *Shank2*$^{-/-}$ (right) mice (paired t-test, n = 19 sessions from 7 WT mice, n = 18 sessions from 6 *Shank2*$^{-/-}$ mice, $p < 0.001$ for WT, $p < 0.05$ for *Shank2*$^{-/-}$). Circles of the same color indicate sessions from the same mouse.

(**B**) Comparison of *d'* of the signal detection theory (unpaired t-test, n = 19 sessions for WT, n = 18 sessions for *Shank2*$^{-/-}$, $p < 0.05$). Circles of the same color indicate sessions from the same mouse.

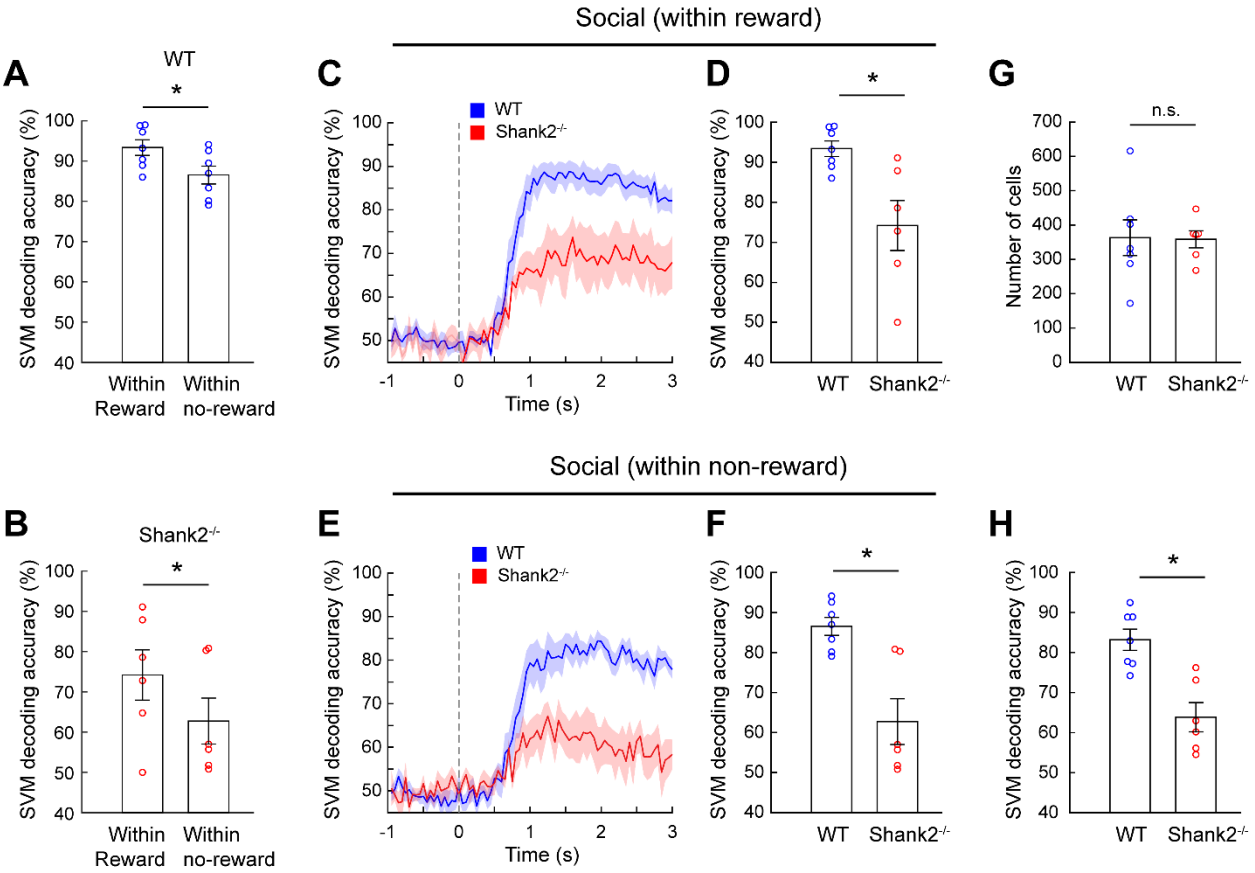


**Figure S4 Comparison of SVM decoding accuracies for social information in reward versus non-reward categories.**

(**A**) SVM decoding accuracies for social information within reward or non-reward trials in WT (paired t-test, n = 7, $p < 0.01$).

(**B**) SVM decoding accuracies for social information within reward or non-reward trials in *Shank2*$^{-/-}$ mice (paired t-test, n = 6, $p < 0.05$).

(**C**) SVM decoding accuracies for social information within reward trials in WT and *Shank2*$^{-/-}$ mice.

(**D**) Comparison of the SVM decoding accuracies for social information within reward trials (unpaired t-test, n = 7 for WT, n = 6 for *Shank2*$^{-/-}$, $p < 0.01$).

(**E**) SVM decoding accuracies for social information within non-reward trials in WT and *Shank2*$^{-/-}$ mice.

(**F**) Comparison of the SVM decoding accuracies for social information within non-reward trials (unpaired t-test, n = 7 for WT, n = 6 for *Shank2*$^{-/-}$, $p < 0.01$).

(**G**) Comparison of the number of cells used for SVM decoding after reward learning in WT and *Shank2*$^{-/-}$ mice (unpaired t-test, n = 7 for WT, n = 6 for *Shank2*$^{-/-}$, $p = 0.94$).

(**H**) Comparison of the SVM decoding accuracies for social information after reward learning, matching the number of cells between WT and *Shank2*$^{-/-}$ mice (unpaired t-test, n = 7 for WT, n = 6 for *Shank2*$^{-/-}$, $p < 0.01$).

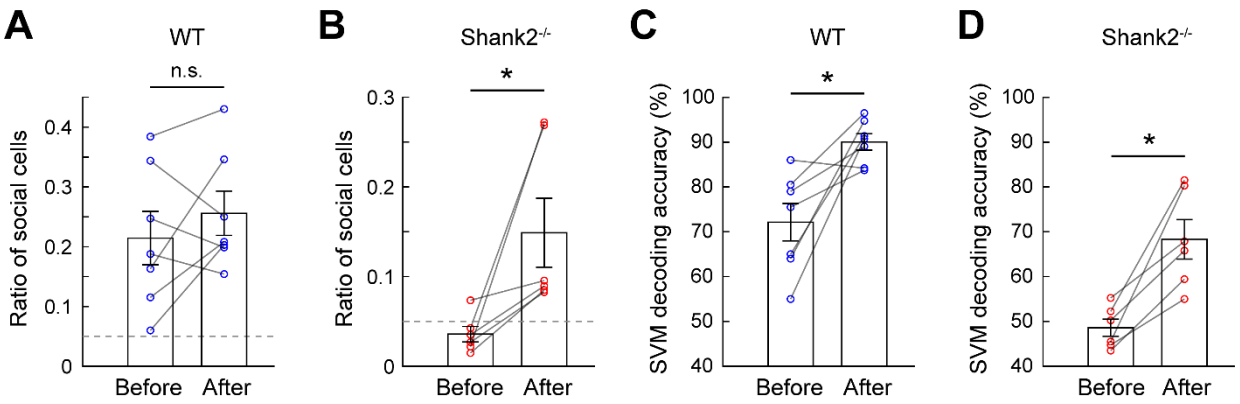


**Figure S5 Within-subject comparison of the ratio of social cells and the SVM decoding accuracies before and after reward learning in WT and *Shank2*$^{-/-}$ mice tested in both conditions.**

(**A**) Comparison of the ratio of social cells during passive presentation before and after reward learning in WT mice (paired t-test, n = 7, p = 0.49).

(**B**) Comparison of the ratio of social cells during passive presentation before and after reward learning in *Shank2*$^{-/-}$ mice (paired t-test, n = 6, $p < 0.05$).

(**C**) Comparison of the SVM decoding accuracies for social information before and after reward learning in WT mice (paired t-test, n = 7, $p < 0.01$).

(**D**) Comparison of the SVM decoding accuracies for social information before and after reward learning in *Shank2*$^{-/-}$ mice (paired t-test, n = 6, $p < 0.01$).

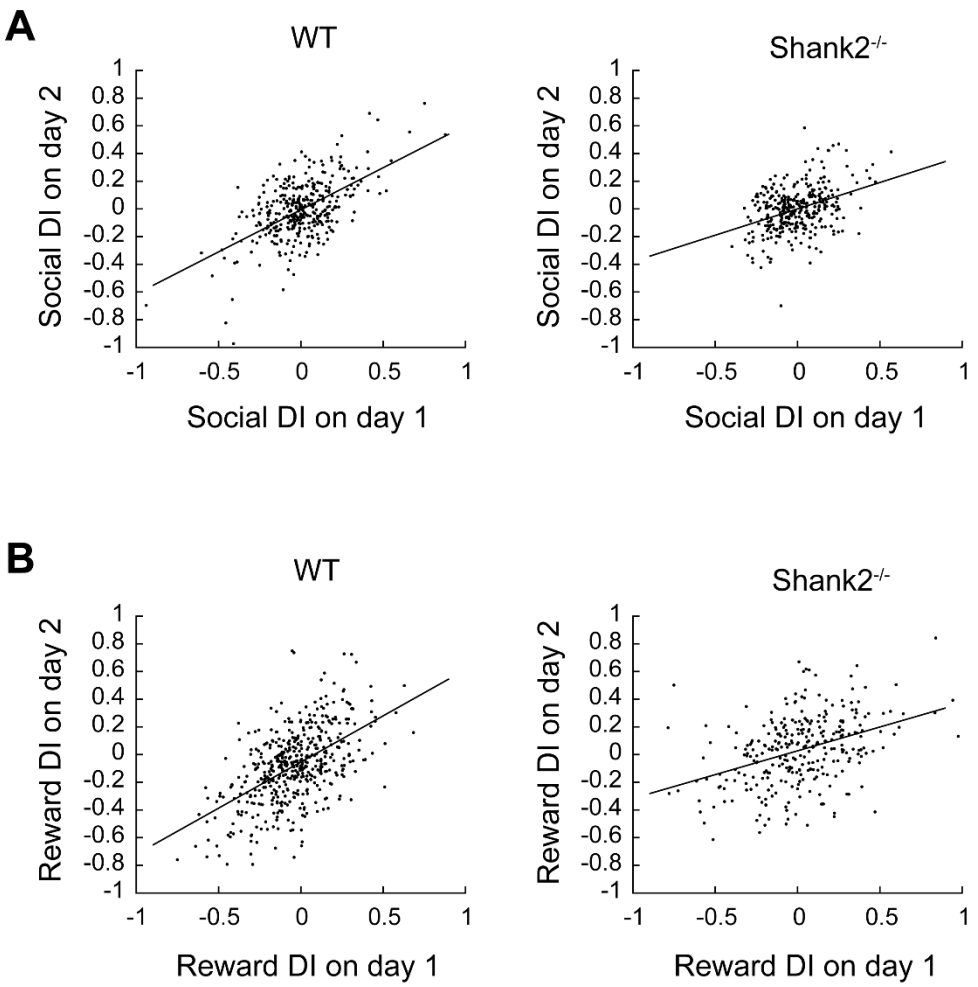


**Figure S6 Comparison of stabilities of social and reward representations between WT and *Shank2*$^{-/-}$ mice.**

(**A**) Correlation of discrimination index (DI) values for social information in two successive daily sessions in example WT (left, $r = 0.60$, $p < 0.001$) and *Shank2*$^{-/-}$ (right, $r = 0.38$, $p < 0.001$) mice. Dots indicate individual neurons.

(**B**) Correlation of DI values for reward information in two successive daily sessions in example WT (left, $r = 0.55$, $p < 0.001$) and *Shank2*$^{-/-}$ (right, $r = 0.42$, $p < 0.001$) mice.

| Animal ID | Genotype | # of Cells | Social | Non-specific |
|---|---|---|---|---|
| 1 | WT | 276 | 106 | 170 |
| 2 | WT | 410 | 77 | 333 |
| 3 | WT | 286 | 59 | 227 |
| 4 | WT | 477 | 55 | 422 |
| 5 | WT | 233 | 38 | 195 |
| 6 | WT | 348 | 70 | 278 |
| 7 | WT | 450 | 27 | 423 |
| 8 | WT | 320 | 110 | 210 |
| 9 | WT | 352 | 87 | 265 |
| 10 | *Shank2*$^{-/-}$ | 273 | 6 | 267 |
| 11 | *Shank2*$^{-/-}$ | 343 | 27 | 316 |
| 12 | *Shank2*$^{-/-}$ | 305 | 13 | 292 |
| 13 | *Shank2*$^{-/-}$ | 404 | 6 | 398 |
| 14 | *Shank2*$^{-/-}$ | 299 | 22 | 277 |
| 15 | *Shank2*$^{-/-}$ | 335 | 9 | 326 |
| 16 | *Shank2*$^{-/-}$ | 253 | 6 | 257 |
| 17 | *Shank2*$^{-/-}$ | 284 | 10 | 274 |

**Table S1 A summary table of the dataset used for passive presentation.**

| Animal ID | Genotype | # of Cells | Social | Reward | Both | Non-specific | Interaction |
|---|---|---|---|---|---|---|---|
| 1 | WT | 172 | 66 | 15 | 8 | 77 | 6 |
| 2 | WT | 402 | 52 | 19 | 10 | 292 | 29 |
| 4 | WT | 418 | 58 | 79 | 29 | 161 | 91 |
| 5 | WT | 315 | 95 | 28 | 14 | 155 | 23 |
| 7 | WT | 616 | 100 | 61 | 25 | 372 | 58 |
| 8 | WT | 288 | 51 | 41 | 21 | 142 | 33 |
| 9 | WT | 332 | 39 | 60 | 27 | 149 | 57 |
| 10 | *Shank2*$^{-/-}$ | 375 | 66 | 53 | 36 | 179 | 41 |
| 12 | *Shank2*$^{-/-}$ | 372 | 54 | 84 | 46 | 129 | 59 |
| 13 | *Shank2*$^{-/-}$ | 447 | 29 | 71 | 9 | 307 | 31 |
| 14 | *Shank2*$^{-/-}$ | 314 | 16 | 52 | 14 | 220 | 12 |
| 15 | *Shank2*$^{-/-}$ | 375 | 20 | 63 | 11 | 253 | 28 |
| 17 | *Shank2*$^{-/-}$ | 268 | 15 | 59 | 9 | 154 | 31 |

**Table S2 A summary table of the dataset used for after reward learning.**

| Animal ID | Genotype | # of Cells | Social | Non-specific |
|---|---|---|---|---|
| 10 | *Shank2*$^{-/-}$ | 389 | 28 | 361 |
| 12 | *Shank2*$^{-/-}$ | 342 | 26 | 316 |
| 13 | *Shank2*$^{-/-}$ | 370 | 30 | 340 |
| 14 | *Shank2*$^{-/-}$ | 386 | 49 | 337 |
| 15 | *Shank2*$^{-/-}$ | 548 | 10 | 538 |
| 17 | *Shank2*$^{-/-}$ | 242 | 24 | 218 |

**Table S3 A summary table of the dataset used for passive presentation after reward learning.**